C. R. Mecanique 345 (2017) 271–280

Contents lists available at ScienceDirect

Comptes Rendus Mecanique

www.sciencedirect.com

Fatigue crack growth simulation in coated materials using X-FEM

Khalid Nasri *, Mohammed Zenasni

Équipe de mécanique et calcul scientifique, ENSA, Université Mohamed-1er, BP 696, Oujda, Maroc

A R T I C L E   I N F O

Article history:
Received 16 November 2016
Accepted 24 February 2017
Available online 17 March 2017

Keywords:
Fatigue life
Crack growth rate
XFEM
Bi-material
Propagation
Two cracks

A B S T R A C T

In the present work, the eXtended Finite Element Method (XFEM) is used to study the effect of bi-material interfaces on fatigue life in galvanised panels. X-FEM and Paris law are implemented in ABAQUS software using Python code. The XFEM method proved to be an adequate method for stress intensity factor computation, and, furthermore, no remeshing is required for crack growth simulations. A study of fatigue crack growth is conducted for several substrate materials, and the influence of the initial crack angle is ascertained. This study also compares the crack growth rate between three types of bi-materials alloys zinc/steel, zinc/aluminium, and zinc/zinc. The interaction between two cracks and fatigue life, in the presence of bi-material interface, is investigated as well.

1. Introduction

Due to the increase in material costs, many steel manufacturers start to protect steel against corrosion in order to extend its life and to provide more reliable and enduring products. For this purpose, several protection categories are used. The best option in terms of quality/price ratio is the utilisation of galvanised steel plates for car bodies. The galvanising process consists in dipping the steel sheets in a hot bath of zinc for a sufficient time to allow a metallurgical reaction between the steel surface and the molten zinc. Indeed, a protective layer of zinc covers both sides of the galvanised steel and drastically reduces corrosion. In addition, the plates of the vehicles are subjected to complex and cyclic loading combinations due to severe operational conditions. These combinations are at the origin of the starting and the propagation of cracks in these parts, which can lead to fracture [1,2]. For this reason, it is very interesting, through a numerical modelling based on a coupling of X-FEM and Paris law, to describe the fatigue crack growth behaviour in automobile parts. The fatigue crack growth phenomenon has been studied from different points of view by several authors. Paris and Erdogan [3] established an empirical relation between the crack propagation rate and applied stress intensity factors range for crack growth analysis called Paris law. Walker [4] modified the Paris law equation by considering the mean stress effect. Elber [5] used an equivalent stress intensity factor to take into account crack closure under compression. A homogenised XFEM approach has been proposed by [6] to evaluate the fatigue life of an edge crack plate in the presence of discontinuities. Chan [7] has developed a fatigue crack initiation model based on microstructure, which includes explicit crack size and microstructure scale parameters. Fatigue life prediction and crack growth simulation have been studied by the extended finite element method [8–11].

* Corresponding author. Fax: +212 536505472.
E-mail address: Prof.nasri@gmail.com (K. Nasri).

http://dx.doi.org/10.1016/j.crme.2017.02.005
1631-0721/

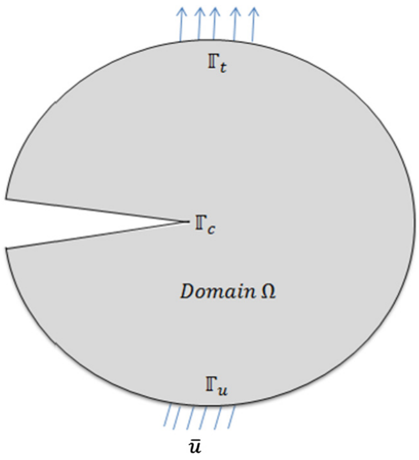

Fig. 1. Description of the problem.

Pathak et al. [9] coupled the Paris law and the element-free Galerkin method to simulate the fatigue crack growth of homogeneous and bi-material interfacial cracks. Ritchie [12] examined the mechanisms of fatigue crack propagation in ductile and brittle solids.

Mazière and Fedelich [13] simulated 2D fatigue crack propagation using the finite element method and implementation of the strip-yield model. Shi and Zhang [14] simulated the interfacial crack growth of fiber-reinforced composites under tension–tension cyclic loading using the finite element method. In their model, the energy release rate is calculated and utilised in the Paris law in order to calculate crack growth rate.

Moreover, an accurate evaluation of stress intensity factor (SIFs) is quite essential for the prediction of failure and crack growth. To evaluate the stress intensity factor of a cracked component, numerical tools such as finite element method (FEM) [15], boundary element method [16], and extended finite element method (XFEM) [16–18] are available. Out of these numerical methods, the extended finite element method has been found to be the most successful and powerful numerical method for solving variety of engineering and science problems. In this method (XFEM), standard finite element approximation is enriched locally with some additional functions [19], which are obtained from the theoretical background of the problem. In this method, a crack can be modelled independently of the finite element mesh. To track a moving discontinuity (crack growth) the level set method is proposed by [20] and was first applied in XFEM by [20,21]. The interaction between bi-material interface with a crack was modelled by the XFEM method [22–24] and examined by several authors [25–28]. The extended finite element method for fracture problems is implemented in ABAQUS software [29] by UEL subroutine.

The present paper focuses on the study of interface effects on the fatigue crack growth in galvanised panels. To this aim, an extended finite element method is coupled with the Paris Law and implemented in ABAQUS software [30] using the Python code.

The paper is organised as follows: Section 2 highlights the discretisation and governing equation of linear elasticity. The fatigue life calculation and the formulation XFEM are also recalled in this section. In the last sections, the numerical method is validated and used to study the effect of interfaces and mechanical properties of substrate on the fatigue crack growth. The interaction between two cracks and inclined crack effect are also touched upon.

2. Numerical formulation

2.1. Discretisation and governing equations

Considering a body Ω with the boundary Γ show Fig. 1. The partial differential equation and boundary conditions for a linear solid mechanics problem can be written as follows [31–33]:

$$\nabla \cdot \sigma + b = 0 \quad \text{in } \Omega \tag{1}$$

$$\sigma \cdot n = \bar{t} \quad \text{on } \Gamma_t \tag{2}$$

$$u = \bar{u} \quad \text{on } \Gamma_u \tag{3}$$

$$\sigma \cdot n = 0 \quad \text{on } \Gamma_c \tag{4}$$

where σ is Cauchy stress tensor, n is the unit outward normal to Ω, $\bar{u}$ and $\bar{t}$ are the prescribed displacements and tractions, respectively, and Γ_t, Γ_u and Γ_c are the traction, displacement and crack boundaries, respectively, and b is the body force.

Based on Eqs. (1)–(4), the variational form of the equilibrium equation can be written as:

$$\int_{\Omega} \sigma \cdot \varepsilon \mathrm{d}\Omega = \int_{\Omega} b \cdot \delta u \mathrm{d}\Omega + \int_{\Gamma} \bar{t} \cdot \delta u \mathrm{d}\Gamma \tag{5}$$

The discretisation of Eq. (5) using the procedure of Eq. (7) results in a discrete system of linear equilibrium equations for each node,

$$K^e u^e = f^e \tag{6}$$

where K^e is the nodal stiffness matrix, u^e is the nodal vector of degrees of nodal freedom for both classical and enriched ones, and f^e is the nodal vector of external force. The detail of matrix K^e and f^e can be referred to reference [34].

2.2. XFEM formulation

In the standard two-dimension XFEM formulation, the total displacement $u(x)$ at the point of location x within element is approximated by:

$$u(x) = \sum_{i=1}^{N} N_i(\boldsymbol{x}) u_i + \sum_{i \in W_b} N_i(\boldsymbol{x}) H(\boldsymbol{x}) a_i + \sum_{i \in W_s} \sum_{j=1}^{4} N_i(\boldsymbol{x}) \gamma_j(\boldsymbol{x}) b_{ji} \tag{7}$$

where N_i are the standard finite element shape functions, u_i the nodal displacements of the element, and n is the global nodes number. Nodes of an element are completely and partially cut by the crack are represented by W_b and W_s, respectively. a_i is the nodal enriched degree of freedom associated with the Heaviside function. b_{ij} is the nodal enriched degrees of freedom vector associated with the crack-tip enrichment function.

The Heaviside function H is a discontinuous function through the crack surface and is constant on each side of the crack. Finally, $\gamma_j(x)$ is the crack tip enrichment function, which can be written as [31]:

$$\gamma_j(x) = \left[\sqrt{r}\sin\frac{\theta}{2}, \sqrt{r}\cos\frac{\theta}{2}, \sqrt{r}\sin\frac{\theta}{2}\cos\theta, \sqrt{r}\cos\frac{\theta}{2}\cos\theta\right] \tag{8}$$

2.3. Fatigue life calculation

In this section, the criterion for fatigue crack growth direction is concisely detailed. The fatigue crack propagation simulation is performed by XFEM under constant amplitude cyclic loading. When the discrete equations [35] are solved and the values of SIFs are extracted. The range of SIF for constant amplitude cyclic loading is defined as:

$$\Delta K = K_{\max} - K_{\min} \tag{9}$$

where $K_{\max}$ and $K_{\min}$ are the stress intensity factors corresponding to the maximum and minimum applied loads, respectively. In reality, the crack path is curved, so the crack is simulated by successive linear segments increments. It is necessary to determine the direction of crack growth and the length of these increments. Some criteria allow one to determine the crack growth direction under cyclic loading. Here, the maximum principal stress criterion is used, which imposes that the crack grows in the direction of the maximum circumferential stress.

The direction of crack growth θ_c at each crack increment is obtained by the following expression [36]:

$$\theta_c = 2\arctan\frac{1}{4}\left(\frac{K_{\mathrm{I}}}{K_{\mathrm{II}}} - \mathrm{sign}(K_{\mathrm{II}})\sqrt{\left(\frac{K_{\mathrm{I}}}{K_{\mathrm{II}}}\right)^2 + 8}\right) \tag{10}$$

where K_{I} and K_{II} are respectively mode I and mode II stress intensity factors. For quasi-static analysis, the fatigue life is obtained using the generalised Paris law [37]:

$$\frac{\mathrm{d}a}{\mathrm{d}N} = C(\Delta K)^m \tag{11}$$

where a is the crack length, N is the number of loading cycles, C and m are material constants.

The formulation of the ΔK range is proposed by Tanaka [38]:

$$\Delta K = \sqrt[4]{K_{\mathrm{I}}^4 + 8K_{\mathrm{II}}^4} \tag{12}$$

The incremental crack growth length is given by:

$$\Delta a = C \cdot N \cdot (\Delta K)^m \tag{13}$$

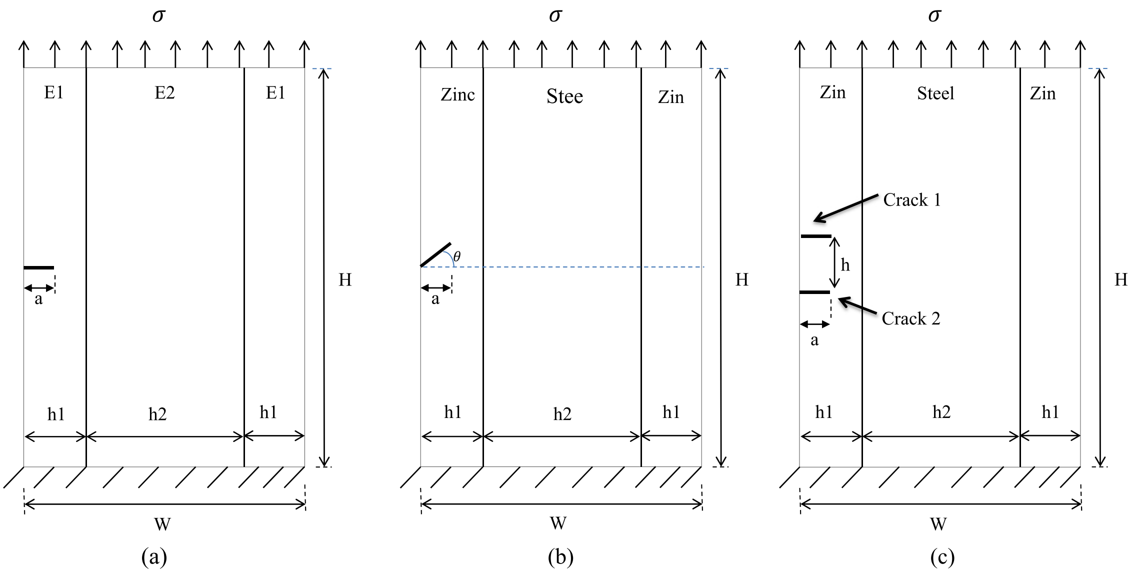

Fig. 2. Geometry and general notation of the bi-material model considered for different cases. (a) Perpendicular crack and with different substrate materials. (b) Inclined edge crack with a different angle θ in the zinc/steel bi-material. (c) Two parallel edge cracks with the same length in the zinc/steel bi-material.

Table 1
Mechanical properties of zinc and steel.

Material	Elastic modulus [GPa]	Poisson's ratio
Steel TRIP800	210	0.3
Zinc	100	0.3

3. Finite element model and materials properties

The bi-material rectangular plate considered in this investigation has the following dimensions: height $H = 30$ mm and width $W = 20$ mm. The plate is subjected to a cyclic tensile loading of $\sigma_{min} = 0$ MPa and $\sigma_{max} = 100$ MPa. The dimensions of the coating and the base material are $h_1 = 0.08$ mm and $h_2 = 19.84$ mm, respectively, as shown in Fig. 2a.

The mechanical properties of the two materials are presented in Table 1. The SIFs analyses were performed using the XFEM method [30]. The type of mesh elements used consists of Four Node bilinear Quadrilateral Elements and the element size around the crack and interface zone is about 1 μm. A convergence study with varying nodes number is realised until mesh-independent results are attained.

4. Numerical results and discussion

In this section, four numerical examples are shown. In the first example, the accuracy of the implemented method is tested by calculating the Stress Intensity Factor for different crack lengths in an infinite plate. The obtained numerical results are compared with those of the literature [39,40]. In the second example, a single edge crack in a rectangular bi-material is considered: the effects of the mechanical properties on the fatigue life and crack propagation rate are studied. In the third example, the effect of crack orientation on the fatigue life is studied, thus its effect on the crack growth rate.

Finally, the effect of interaction between two cracks on the crack propagation rate in the zinc/steel bi-material is also investigated.

4.1. Edge crack in an infinite plate

To validate the implementation of the XFEM method using the python code in Abaqus software, a single edge crack in infinite plate under uniaxial tension is considered. The crack length is varied from 20 μm to 70 μm. The Young's modulus and Poisson's ratio are equal 210 GPa and 0.3 respectively. The analytical expression of the K_I SIF of this problem is expressed as a function of a shape coefficient $f(\frac{a}{w})$:

Table 2
Error in the computation of the shape coefficient for an infinite plate.

Crack length [mm]	$f(\frac{a}{w})$ [39,40]	Numerical $f(\frac{a}{w})$	Error (%)
0.02	1.12178	1.12081	0.08600
0.03	1.12168	1.12031	0.12175
0.04	1.12158	1.11987	0.15226
0.05	1.12149	1.11959	0.16910
0.06	1.12140	1.11945	0.17369
0.07	1.12132	1.11942	0.16956

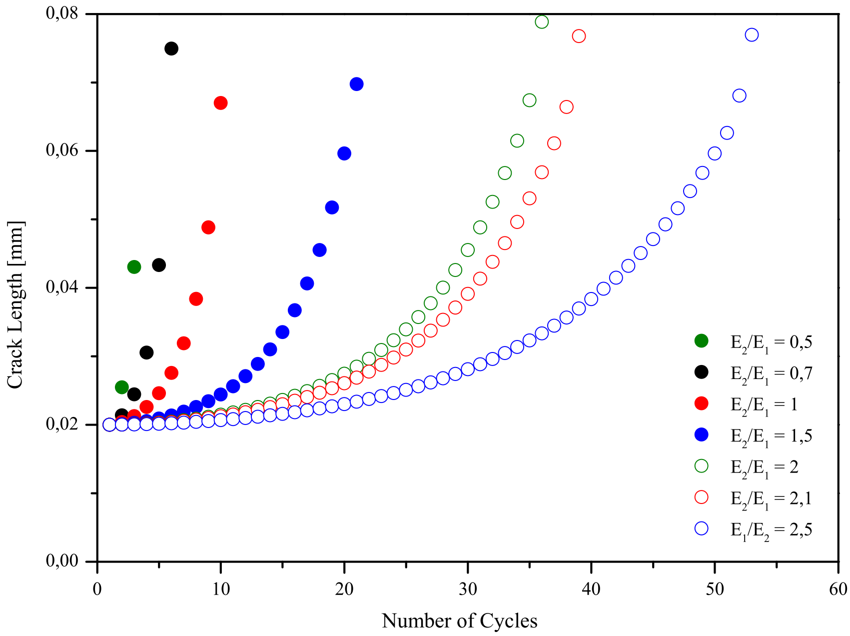

Fig. 3. Fatigue life variation with crack length for various E_2/E_1 ratios.

$$K_I = f\left(\frac{a}{w}\right)\sigma\sqrt{\pi a} \tag{14}$$

$$f\left(\frac{a}{w}\right) = 1.112 - 0.231\left(\frac{a}{w}\right) + 10.550\left(\frac{a}{w}\right)^2 - 21.71\left(\frac{a}{w}\right)^3 + 30.382\left(\frac{a}{w}\right)^3 \tag{15}$$

The obtained results are reported in Table 2 and compared to the solution given in [39,40], a good agreement is found.

4.2. Bi-material interface effects

To investigate the effect of the mechanical properties of the substrate on fatigue crack growth, the E-modulus of the coating is constantly fixed, unlike the substrate – it is varied. Two actual configurations corresponding to the galvanised zinc/steel and zinc/aluminium will be highlighted since they are most often used in the automotive sector. A plate formed by a zinc/substrate bi-material is considered (Fig. 2a). A perpendicularly edge crack to the interface is located in the zinc.

Fig. 3 shows the dependence of the crack length on the number of cycles for various substrate materials. It is clearly observed that the rigidity of the substrate material has a substantial effect on the behaviour of the crack initially located in the coating. Indeed, the number of cycles is found to decrease when the rigidity of the substrate decreases.

The effect of rigidity is expressed by the ratio between the E-modulus of the substrate and that of the coating materials. For instance, when this ratio is equal to 0.5, the crack approaches the interface with a very low number of cycles, namely 3. This number increases until the number of 53 cycles for a rigidity ratio of $\frac{E_2}{E_1} = 2.5$. These results also show that the fatigue life of the plate is reduced and elevated with substrate rigidity. For example, the fatigue life in bi-material zinc/aluminium and zinc/steel panels is reduced and elevated by 65% and 235% respectively, in comparison with the homogeneous material zinc/zinc. This behaviour is related to the rigidity of the substrate that resists crack opening.

The presence of an interface has a marked effect on the crack growth. For this purpose, the dependence of the crack growth rate $\frac{da}{dN}$ on the value of ΔK is determined and plotted in Fig. 4 for different rigidity ratio $s\frac{E_2}{E_1}$. To check the effect of a softer substrate on the crack growth behaviour, the crack growth rate of a zinc/aluminium bi-material is evaluated and

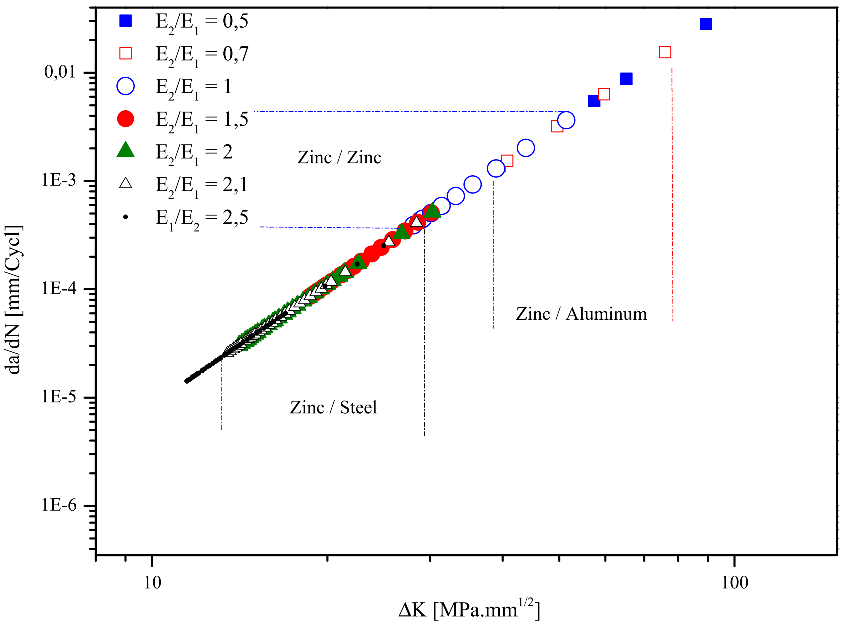

Fig. 4. Crack growth rate variation with ΔK range for various E_2/E_1 ratios.

inserted in the figures for comparison. The configurations zinc/aluminium, zinc/zinc and zinc/steel, most encountered in the industrial sector, are highlighted by a dotted line.

The apparent variation of the crack growth rate and the fatigue life in the three configurations are noted. The presence of the interface may have a beneficial or harmful effect depending on whether the substrate is stronger or softer. When the second material is softer, a higher stress field is developed around of crack tip and the interface. Under this effect, the crack is rapidly propagated towards the substrate, and its fatigue life is reduced (see Fig. 3).

Inversely, when the second material is stiffer than the first one, the crack tends to deviate to avoid the interface and to propagate with a low speed. Furthermore, when the ratio between the E-modulus of the substrate and the coating materials is important, the crack tends to grow far from the bi-material interface.

For instance, in the panel composed by zinc/aluminium bi-material, the crack is spread quickly in comparison with the zinc/steel bi-material. This result implies that in zinc/steel panel, the crack is delayed and blocked by the rigidity of the steel.

4.3. Inclined crack with different orientations

In real problems, the crack is not always normal to the bi-material interface. It may deviate due to the rigidity of the interface. This is why the examination of cracks with different angles should complete the universal and classic case where the crack is perpendicular to the interface. In this regard, the same plate as that presented in the precedent section is considered. An inclined crack at the interface is located in the zinc coating with different orientations (Fig. 2b).

The effect of the initial orientation of the crack on the fatigue life of the panels is discovered. For that, the obtained results in terms of the variation of crack length as a function of number of cycles for different crack orientations are depicted in Fig. 5. Indeed, to approach the bi-material interface, the necessary number of cycle is increased according to the inclination angle θ. This variation is justified by the crack path during propagation. In this case, the crack tends to become perpendicular to the applied load during cycling. This is why the number of cycles required is more significant in comparison with a perpendicular edge crack case.

Fig. 6 shows the variations of $\frac{da}{dN}$ with ΔK for various angles. Note that an orientation angle of 0° corresponds to a crack normal to the interface. It is clearly noticed that the crack propagation rate is affected by the initial orientation of the crack. The results in Fig. 6 show that a crack that is normal to the interface leads to a more significant crack growth rate, and this rate decreases as the angle of orientation increases.

4.4. The interaction between two cracks effect on the fatigue life

In this section, a bi-material zinc/steel is considered (Fig. 2c). The same conditions as those imposed in Section 4 are used. The plate is initiated by two parallel edge cracks, and separated by a distance h. The initial crack length is fixed to 0.02 mm. The mechanical properties of the materials necessary for the computation are summarised in Table 1.

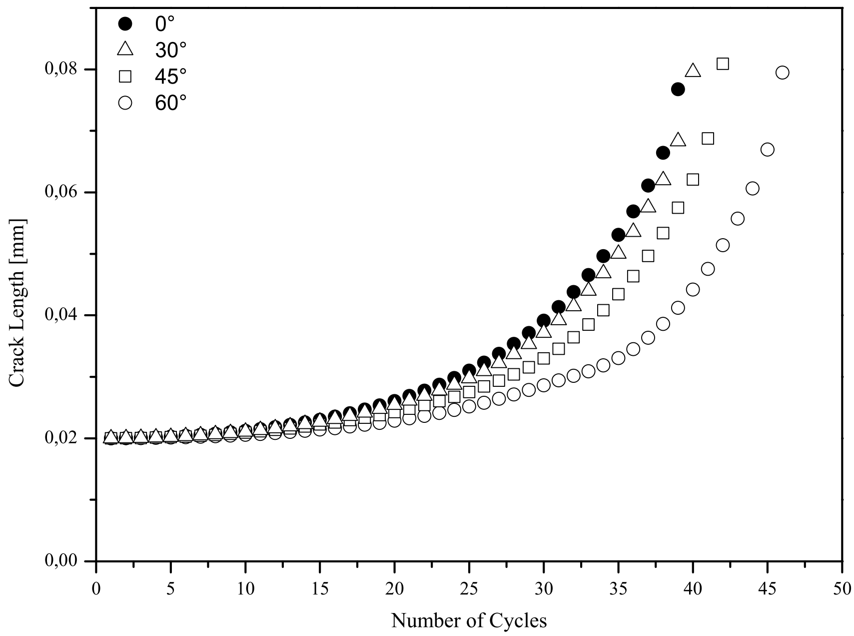

Fig. 5. Fatigue life variation with crack length for different crack orientations.

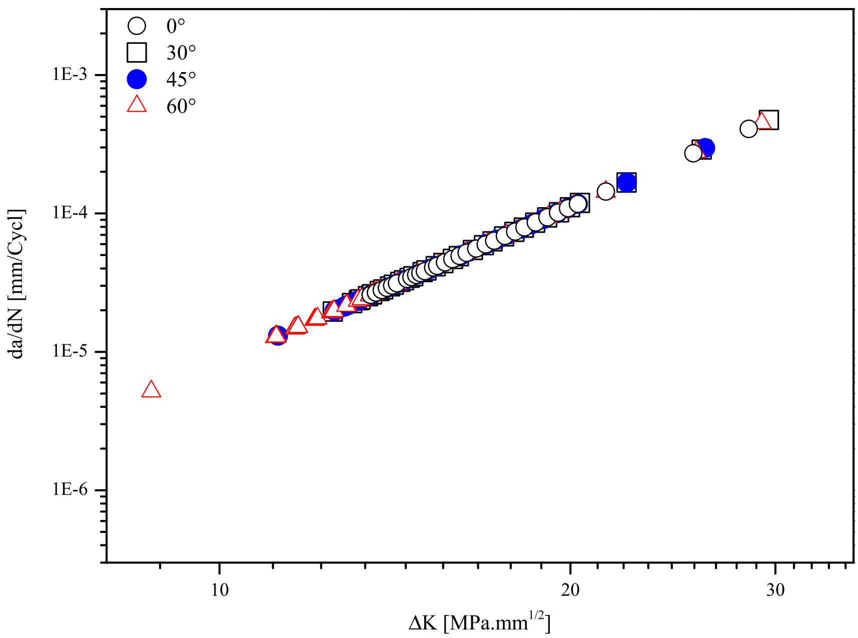

Fig. 6. Dependence of crack growth rate as a function of the ΔK range for different crack orientations.

The distance h between two parallel cracks is progressively changed and the fatigue life corresponding to each crack is numerically computed. The results in Fig. 7 show the variation of the crack length as a function of the number of cycles for different values of the distance h.

The effect of the distance h on the behaviour of the two cracks is well observed. A dominance of crack 2 over crack 1 during propagation when the two cracks are very close to each other ($h = 0.04$ mm) is found. A shift of a number of cycles between two cracks to approach the bi-material interface is noted. This trend is justified by the interaction between the two cracks and the required energy to have the propagation. Moreover, this energy is stored in the structure and consumed by the crack tip in order to be incremented. In terms of crack growth rate, a significant velocity in crack 2 relatively with crack 1 is noticed. This difference is explained by the necessary energy to have double crack propagation (crack 1 and crack 2) is dominated and consumed by crack 2 (see Figs. 7a and 8a).

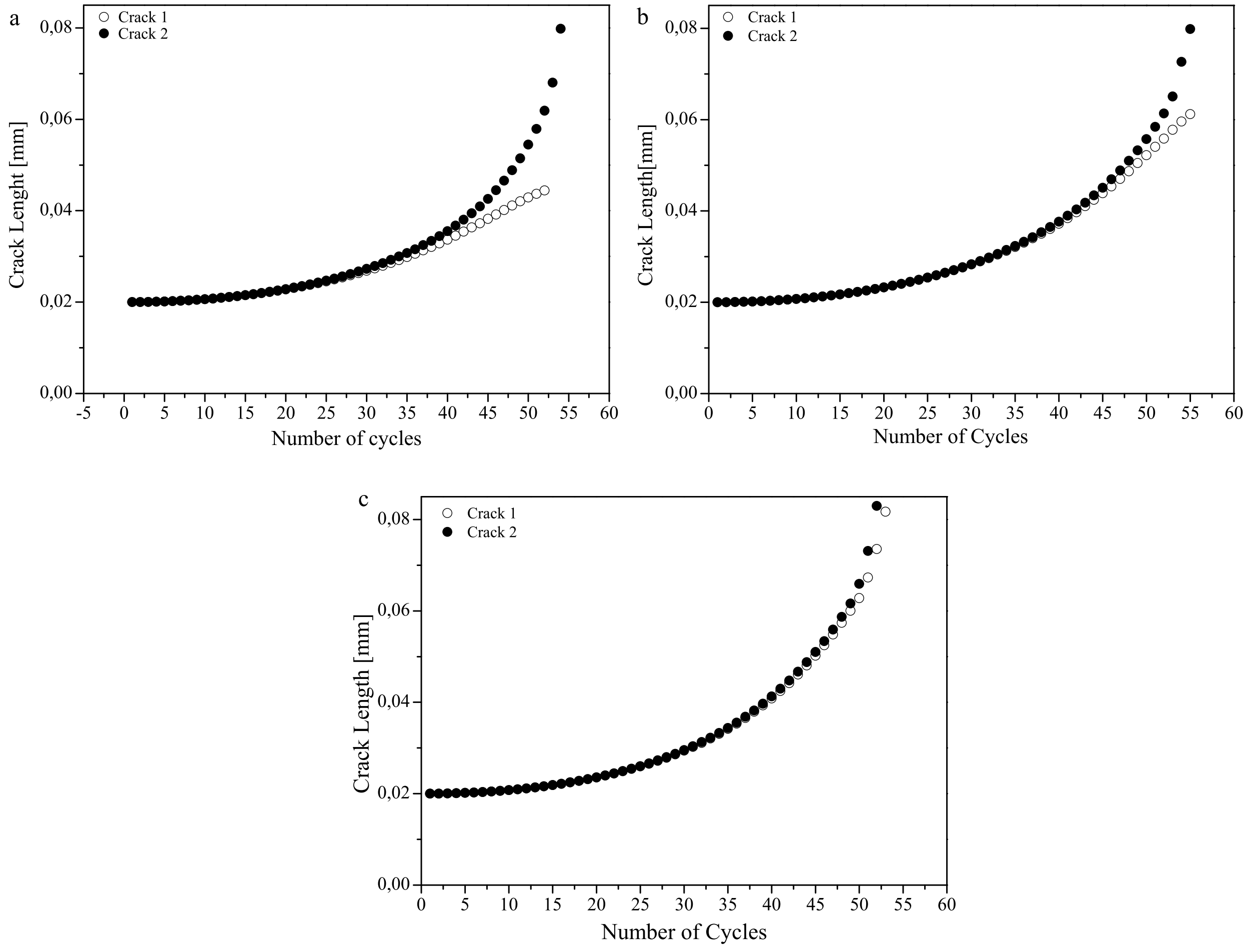

Fig. 7. Fatigue life variation of two cracks with crack length for different distances h: (a) $h = 0.04$ mm, (b) $h = 0.08$ mm, (c) $h = 0.12$ mm.

When the distance h increases, the interaction effect between the cracks decreases up to the value $h = 0.12$ mm; after this distance, the two cracks have the same behaviour as that associated with the single crack case. Moreover, this is why the two cracks have the same crack growth rate and the same way of propagation (see Figs. 7 and Figs. 8). Thus, the results obtained show a good agreement with the available literature result investigation [23].

5. Conclusions

In this study, the eXtended Finite Element Method has been coupled with the Paris law and implemented in ABAQUS software to determine the fatigue life of bi-materials plates. The results obtained in this study yield the following conclusions:

- in the bi-material plate, the rigidity of substrate material has a substantial influence on the cracks behaviour;
- the failure fatigue increases with the decrease of the substrate rigidity;
- in the zinc/aluminium plate, the fatigue life is reduced by 65% in comparison with homogeneous materials;
- the fatigue life is elevated by 235% in a zinc/steel plate than a homogeneous material;
- in the panel composed by the zinc/aluminium bi-material, the crack growth rate is more significant in comparison with a zinc/steel bi-material;
- the failure fatigue decreases when the inclination angle θ increases, and the crack is delayed by the initial slope;
- in the two-crack case, and under fatigue loading boundary conditions, the crack growth rate is significant in one crack in comparison with the other crack when the two cracks are very close to each other;
- when the distance h is considerable ($h > 0.12$ mm), the two cracks have the same growth rate and the same way of propagation.

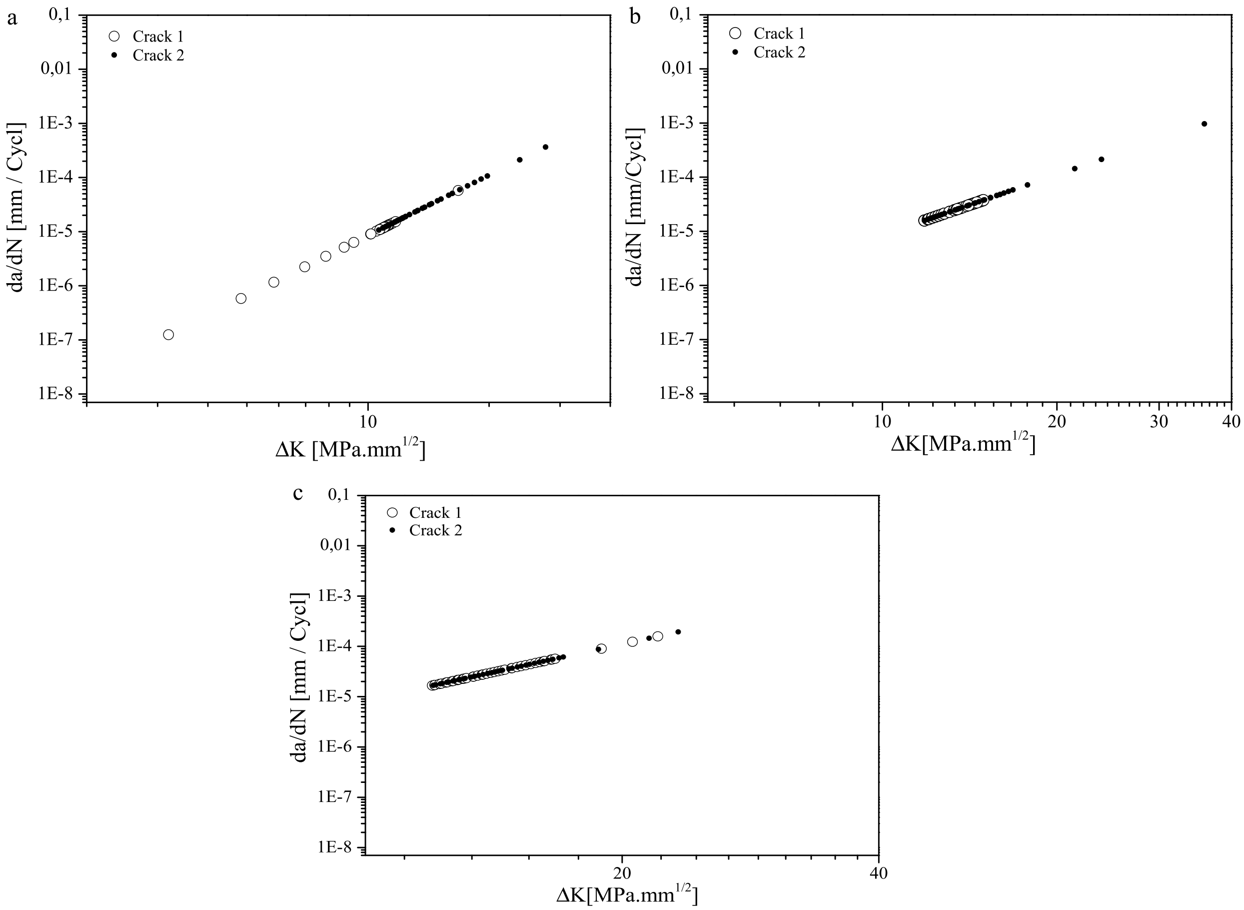

Fig. 8. Crack growth rate variation within the ΔK range for various distances h: (a) $h = 0.04$ mm, (b) $h = 0.08$ mm, (c) $h = 0.12$ mm.

References

[1] A. Chamat, b.S. Aden-Ali, J. Gilgert, E. Petit, K. Nasri, M. Abbadi, Z. Azari, Crack behaviour in zinc coating and at the interface zinc-hot galvanised TRIP steel 800, Eng. Fract. Mech. 114 (2013) 12–25.

[2] K. Nasri, M. Abbadi, M. Zenasni, Z. Azari, Numerical and experimental study of crack behaviour at the zinc/TRIP steel 800 interface, Comput. Mater. Sci. 82 (2014) 172–177.

[3] P.C. Paris, F.A. Erdogan, A critical analysis of crack propagation laws, J. Basic Eng. 85 (1963) 528–533.

[4] E.K. Walker, The effect of stress ratio during crack propagation and fatigue for 2024-T3 and 7076-T6 aluminium, in: Effect of Environment and Complex Load History on Fatigue Life, in: ASTM STR, vol. 462, American Society for Testing and Materials, Philadelphia, PA, USA, 1970, pp. 1–4.

[5] W. Elber, The significance of fatigue crack closure, in: ASTM STR, vol. 486, 1971, pp. 230–242.

[6] S. Kumar, I.V. Singh, B.K. Mishra, A homogenized XFEM approach to simulate fatigue crack growth problems, Comput. Struct. 150 (2015) 1–22.

[7] K.S. Chan, A microstructure-based fatigue-crack-initiation model, Metall. Mater. Trans. A, Phys. Metall. Mater. Sci. 34 (1) (2003) 43–58.

[8] E. Giner, C. Navarro, M. Sabsabi, M. Tur, J. Domínguez, F.J. Fuenmayor, Fretting fatigue life prediction using the extended finite element method, Int. J. Mech. Sci. 53 (3) (2011) 217–225.

[9] P. Himanshu, S. Akhilendra, I.V. Singh, Fatigue crack growth simulations of homogeneous and bi-material interfacial cracks using element free Galerkin method, Appl. Math. Model. 38 (2014) 3093–3123.

[10] S. Bhattacharya, I.V. Singh, B.K. Mishra, Fatigue life simulation of functionally graded materials under cyclic thermal load using XFEM, Int. J. Mech. Sci. 82 (2017) 41–59.

[11] B.K. Hachi, S. Rechak, M. Haboussi, M. Taghite, G. Maurice, C. R. Mecanique 336 (4) (2008) 390–397.

[12] R.O. Ritchie, Mechanisms of fatigue-crack propagation in ductile and brittle solids, Int. J. Fract. 100 (1999) 55–83.

[13] M. Maziere, B. Fedelich, Simulation of fatigue crack growth by crack tip plastic blunting using cohesive zone elements, Proc. Eng. 2 (1) (2010) 2055–2064.

[14] Z. Shi, R. Zhang, Numerical simulation of interfacial crack growth under fatigue load, Fatigue Fract. Eng. Mater. Struct. 32 (2009) 26–32.

[15] L.N. Gifford, P.D. Hilton, Stress intensity factors by enriched finite elements, Eng. Fract. Mech. 10 (1978) 485–496.

[16] S.T. Raveendra, P.K. Banerjee, Boundary element analysis of cracks in thermally stresses planar structures, Int. J. Solids Struct. 29 (1992) 2301–2317.

[17] N. Moës, J. Dolbow, T. Belytschko, A finite element method for crack growth without remeshing, Int. J. Numer. Methods Eng. 46 (1999) 131–150.

[18] M.R. Shirazizadeh, H. Shahverdi, An extended finite element model for structural analysis of cracked beam-columns with arbitrary cross-section, Int. J. Mech. Sci. 99 (99) (2015) 1–9.

[19] T. Belytschko, T. Black, Elastic crack growth in finite elements with minimal remeshing, Int. J. Numer. Methods Eng. 45 (1999) 601–620.

[20] S. Osher, J.A. Sethian, Fronts propagating with curvature-dependent speed: algorithms based on Hamilton–Jacobi formulations, J. Comput. Phys. 79 (1988) 12–49.

[21] M. Stolarska, D.L. Chopp, N. Moes, T. Belytschko, Modeling crack growth by level sets in the extended finite element method, Int. J. Numer. Methods Eng. 51 (2001) 943–960.

[22] N. Sukumar, D.L. Chopp, N. Moes, T. Belytschko, Modeling of holes and inclusions by level sets in the extended finite element method, Comput. Methods Appl. Mech. Eng. 190 (2001) 6183–6200.

[23] K. Nasri, M. Abbadi, M. Zenasni, M. Ghammouri, Z. Azari, Double crack growth analysis in the presence of a bi-material interface using XFEM and FEM modelling, Eng. Fract. Mech. 132 (2014) 189–199.

[24] L. Bouhala, Q. Shao, Y. Koutsawa, A. Younes, P. Nunez, A. Makradi, et al., An XFEM crack-tip enrichment for a crack terminating at a bi-material interface, Eng. Fract. Mech. 102 (2013) 51–64.

[25] H. Pathak, A. Singh, I.V. Singh, Fatigue crack growth simulations of bi-material interfacial cracks under thermo-elastic loading by extended finite element method, Eur. J. Comput. Mech. 22 (2013) 79–104.

[26] R. Moslemian, A.M. Karlsson, C. Berggreen, Accelerated fatigue crack growth simulation in a bi-material interface, Int. J. Fatigue 33 (2011) 1526–1532.

[27] M.T. Milan, P. Bowen, Experimental and predicted fatigue crack growth resistance in Al2124/Al2124+35% SiC (3 μm) bi-material, Int. J. Fatigue 25 (2003) 649–659.

[28] F. Jiang, Z.L. Deng, K. Zhao, J. Sun, Fatigue crack propagation normal to a plasticity mismatched bi-material interface, Mater. Sci. Eng. A 356 (2003) 258–266.

[29] E. Ginera, N. Sukumar, J.E. Tarancóna, F.J. Fuenmayora, An ABAQUS implementation of the extended finite element method, Eng. Fract. Mech. 76 (3) (2009) 347–368.

[30] ABAQUS/Standard, Documentation for version 6.12. Dassault System Simulia.

[31] S.P. Bordas, P.V. Nguyen, C. Dunant, A. Guidoum, H.N. Dang, An extended finite element library, Int. J. Numer. Methods Eng. 71 (2007) 703–732.

[32] N. Sukumar, D.L. Chopp, N. Moes, T. Belytschko, Modeling of holes and inclusions by level sets in the extended finite element method, Comput. Methods Appl. Mech. Eng. 190 (2001) 6183–6200.

[33] N. Moes, J. Dolbow, T. Belytschko, A finite element method for crack growth without remeshing, Int. J. Numer. Methods Eng. 46 (1999) 131–150.

[34] P. Himanshu, S. Akhilendra, V.S. Indra, Numerical simulation of bi-material interfacial cracks using EFGM and XFEM, Int. J. Mech. Mater. Des. 8 (2012) 9–36.

[35] L. Bouhala, S. Belouettar, A. Makradi, Y. Remond, Study of interface influence on crack growth: application to solid oxide fuel cell like materials design, Mater. Des. 31 (2010) 1033–1041.

[36] C. Shih, R. Asaro, Elastic–plastic analysis of cracks on bimaterial interfaces: part I – small scale yielding, J. Appl. Mech. 55 (1988) 299–316.

[37] P. Paris, M. Gomez, W. Anderson, A rational analytic theory of fatigue, Trend Eng. 13 (1961) 9–14.

[38] K. Tanaka, Fatigue crack propagation from a crack inclined to the cyclic tension axis, Eng. Fract. Mech. 6 (1974) 493–507.

[39] Y. Murakami, Stress Intensity, Factors Handbook Press, Oxford, UK, 1987.

[40] H. Tada, P.C. Paris, G.R. Irwin, Stress Analysis of Cracks Handbook, American Society of Mechanical Engineers, 2001.